Kasprowicz et al., http://www.jcb.org/cgi/content/full/jcb.201310090/DC1

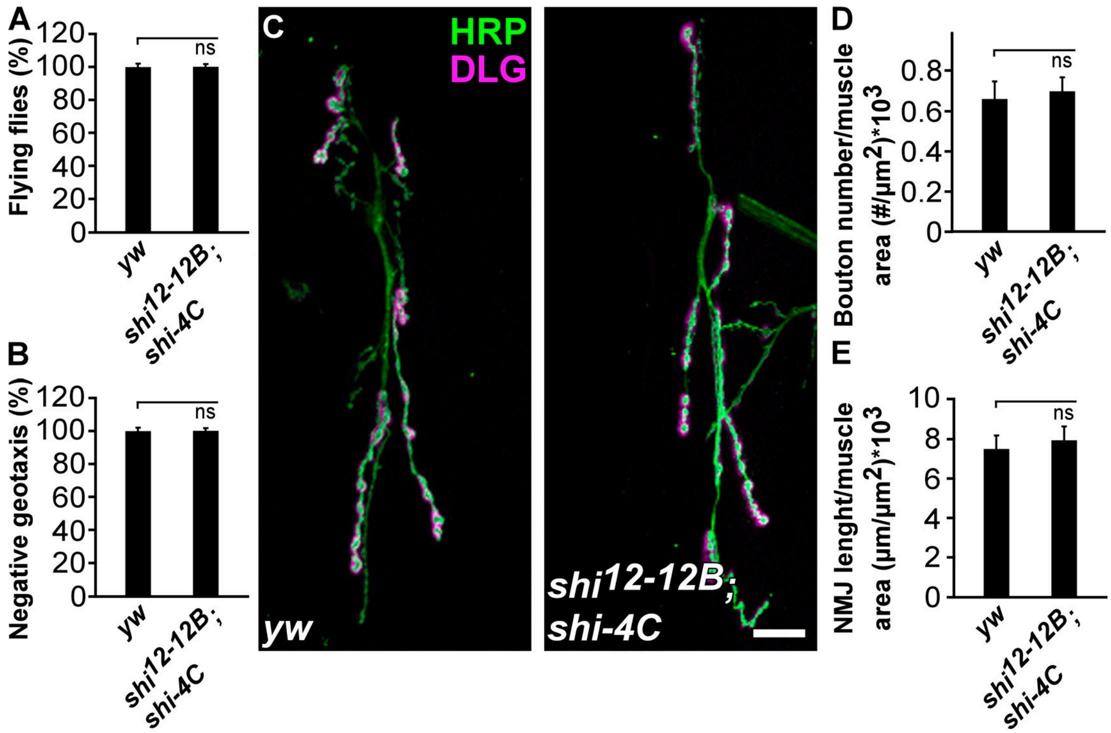

Figure S1. **NMJ morphology of *shi*$^{12-12B}$*; shi-4C* not treated with FALI.** (A and B) *shi*$^{12-12B}$; *shi-4C* are viable and show no obvious behavioral defects, including flight ability (A) and climbing behavior after being tapped down (negative geotaxis; B) as compared with *yw* controls. Error bars show SEMs; *t* test. $n > 40$ flies in groups of five flies. (C) Images of *yw* control and *shi*$^{12-12B}$; *shi-4C* third instar larval fillets at rest labeled with anti-HRP, a presynaptic marker, and anti-DLG, a pre- and postsynaptic marker. Bar, 20 µm. (D and E) Quantification of the bouton number normalized to the muscle area (D) and total NMJ length normalized to the muscle area (E) in *yw* controls and *shi*$^{12-12B}$; *shi-4C* at rest. Error bars show SEMs; *t* test. $n = 6–7$ NMJs from four larvae each.

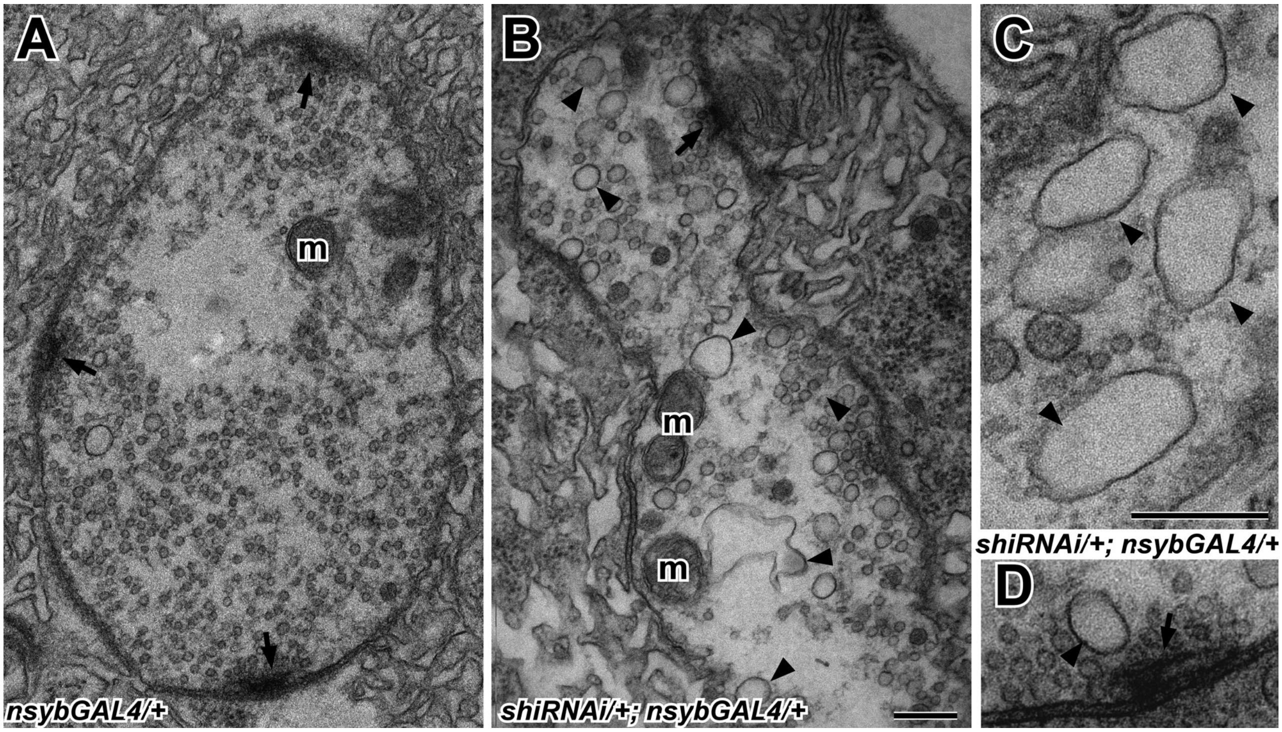

Figure S2. **RNAi-mediated knockdown of Dynamin shows massive membrane internalizations upon stimulation.** (A–D) Electron micrographs of boutons of KCl-stimulated controls (*dicer-2/+;; nSybGal4/+*; A) and larvae expressing *shi* RNAi (*dicer-2/+; shi RNAi/+; nSybGal4/+*; B) as well as larger magnifications of the cisternal invaginations seen upon expression of *shi* RNAi (C) and a presynaptic density in such animals (D). Arrows, active zone; arrowheads, membrane inclusions; m, mitochondria. Bars, 250 nm.

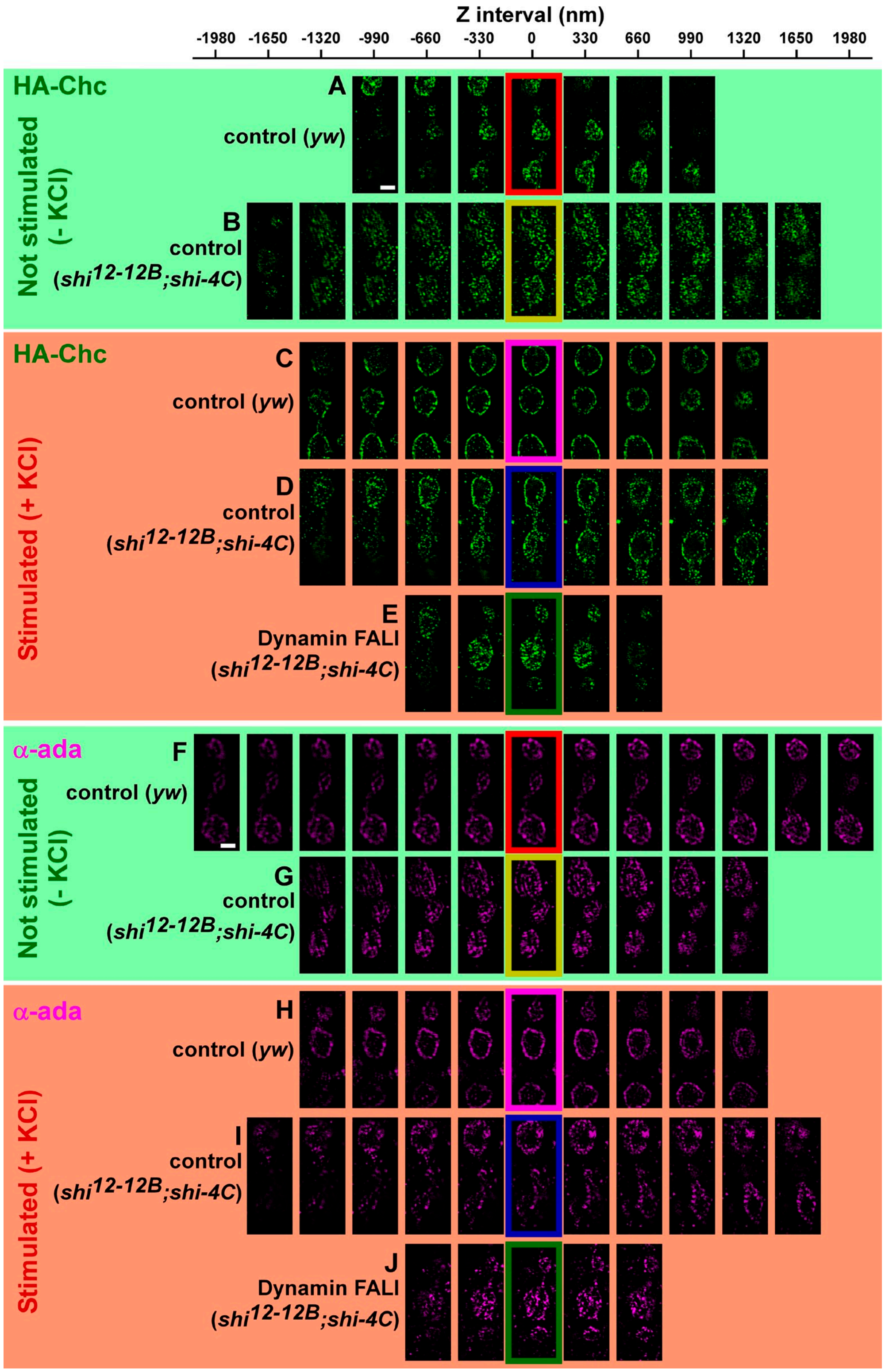

Figure S3. **HA-Chc and α-Ada localization upon Dynamin inactivation.** (A–J) Superresolution imaging of HA-Chc fusion proteins with anti-HA antibodies (A–E) and of α-Ada with antibody labeling (F–J) using structured illumination microscopy and at different z intervals (330 nm for A–G, I, and J and 660 nm for H) through the boutons shown in Fig. 5 (the color coding of the boxed image is identical to Fig. 5) without stimulation (−KCl) and with stimulation (+KCl; 90 mM for 5 min). (A and B) Anti-HA labeling of *yw*; *HA-chc* controls (*yw*, red) and *shi*$^{12\text{-}12B}$/Y; *HA-chc/shi-4C* without FALI (yellow) at rest (−KCl). (C–E) Anti-HA labeling of *yw*; *HA-chc* (*yw*, magenta) and *shi*$^{12\text{-}12B}$/Y; *HA-chc/shi-4C*, stimulated with KCl without Dynamin inactivation (blue; C and D) and with Dynamin inactivation using FALI (green; E). (F and G) Anti–α-Ada labeling of *yw* controls (*yw*, red) and *shi*$^{12\text{-}12B}$/Y; *shi-4C/+* without FALI (yellow) at rest (−KCl). (H–J) Anti–α-Ada labeling of *yw* (*yw*, magenta) and *shi*$^{12\text{-}12B}$/Y; *shi-4C/+*, stimulated with KCl without Dynamin inactivation (blue; H and I) and with Dynamin inactivation using FALI (green; J). Bar, 2 µm.

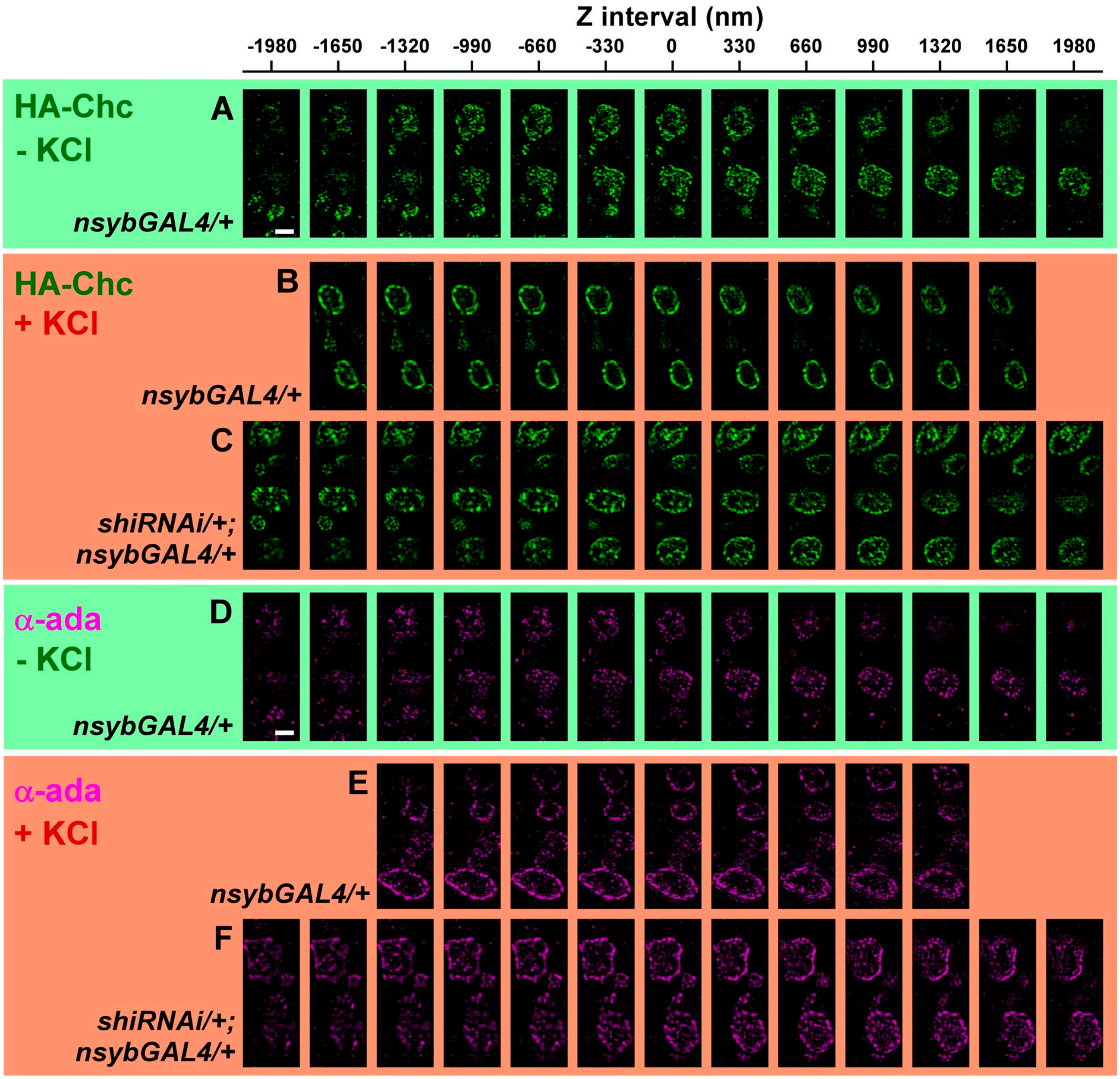

Figure S4. **HA-Chc and α-Ada localization upon RNAi-mediated knockdown of Dynamin.** (A–F) Superresolution imaging of HA-Chc fusion proteins with anti-HA antibodies (A–C) and of α-Ada with antibody labeling (D–F) using structured illumination microscopy and at different z intervals (330 nm) through the boutons that were not stimulated (green, −KCl) or were stimulated (red, +KCl; 90 mM for 5 min) in control animals (*dicer-2/+;; nSybGal4/+*; A, B, D, and E) and in larvae expressing *shi* RNAi (*dicer-2/+; shi RNAi/+; nSybGal4/+*; C and F). Bars, 2 µm.

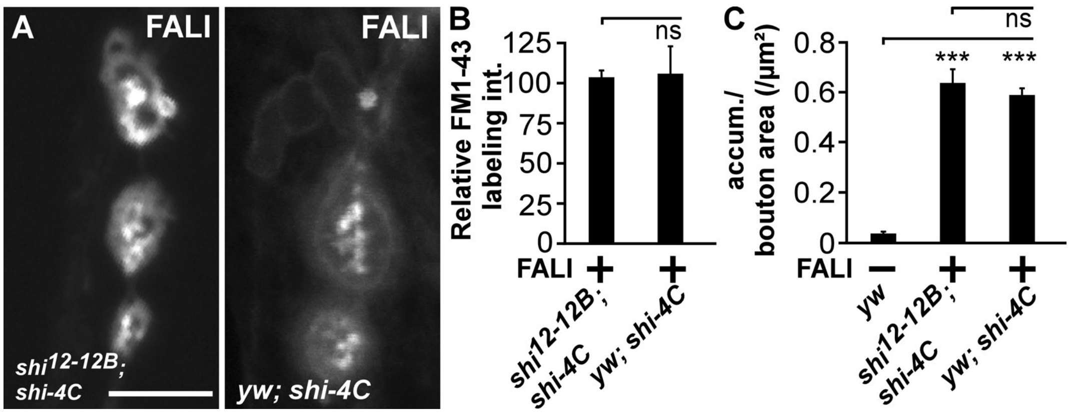

Figure S5. **Shi-4C acts dominantly.** (A) FM 1-43 labeling in *shi*$^{12\text{-}12B}$; *shi-4C* and *yw*; *shi-4C* animals after FALI. Preparations were stimulated with KCl in the presence of FM 1-43 for 5 min, washed, and imaged. Note, large cisternal-like membrane internalizations are also observed in animals expressing Shi-4C in a wild-type background after FALI, indicating that Shi-4C acts dominantly. Bar, 5 µm. (B and C) Quantification of FM 1-43 labeling intensity (int.; n = 32 and 20 boutons from three larvae each) and the number of FM 1-43–labeled accumulations (accum.) per bouton surface area (n = 72, 72, and 32 boutons from 8, 16, and 5 larvae) in *shi*$^{12\text{-}12B}$; *shi-4C* after FALI and *yw*; *shi-4C* after FALI. The labeling intensity is normalized to the control (*shi*$^{12\text{-}12B}$; *shi-4C* after FALI). Error bars show SEMs. (B) t test. (C) ANOVA (post hoc Tukey's test): ***, $P < 0.0001$.

Table S1. **Primers used to create the genomic tagged *shi-4C*, *endo-4C*, and *HA-chc* constructs**

Template vector	Primer name	Primer sequence (5′ → 3′)
Primers used for recombineering-mediated tagging of *shi*		
shi-4C	Dyn_L_term_PL452_R	CATCGCCTGGCTGAAAGTGCTTAAACTCCTCCACCTCCTTCTCCAAAGTACTAGTGGATCCCCTCGAGGGAC
	Dyn_L_Flag_4C_F	CAGGGACACGTTACCTGGCCTGCGGGATAAGTTGCAGAAGCAGATGCTCATGGATTACAAGGATGACGAC
	Dyn_N_reco_F	TCACTATAGGGCGAATTGG
	Dyn_N_reco_R	GAACAAAAGCTGGGTACCGCCC
Primers used for tagging *endoA* with the 4C tag		
endo-4C	Endo F	CTCGACGGTCACGGCGGGCATGTCGAGACTTCGTGCTCGGTACCACTATCGACTGGAAGAATGAGGAAATCGAGG
	Endo 4C R	GAACTCGTTGCGTGGGGGCTCCATGCAGCAGCCGGGGCAGCAATTCAAAAACCGGCTCTCCGCCTCGGAGCGC
	Endo 4C F	GAGGCGGAGAGCCGGTTTTTGAATTGCTGCCCCGGCTGCTGCATGGAGCCCCCACGCAACGAGTTCGTGCCC
	Endo R	GGGTTTTATTAACTTACATACATACTAGAATTCGCATGCCTGCAGTCTAGACCAGGAGCAGGGCGTCTACAAG
Primers used for tagging *chc* with the HA tag		
HA-chc	P[acman]_ura3_AscI_CHC_F	CGAGCGGTCCGTTATCGATGGCGCGCCGGCCTTAATGGCCAGGCGCGCCTAATGAATGAAGGAGTCGTCCTG
	Left_arm_R	CCATCGCTTAACACACAAGATCCTCCTACGCTCCCTCGCTC
	Right_arm_L	CAAGATTATCGCCGTGAGGTAACGATGTAATCGAAGGATTAC
	P[acman]_ura3_CHC_PacI_R	ACAAAAGCTGGGTACCGCCCGGGCGCGATCGCGGCCGGCCACCTTAATTAAAAATTTAGAAACTCACAGATAGC
	Chc_part1_F	CTGGTGTCTGCACCTGTTGGAAACGCTGGATCGTCTGTGGCGTACGCAGAATGGCCTTGG
	Chc_part_1R	CGGATGGGCAGTGGTTGCGTGGCGTAGTCGGGCACGTCGTAGGGGTACATCTTTACTACT
	HA_20_bp_chc_F1	GGCGTAGTCGGGCACGTCGTAGGGGTACATCTTTACTACTACAGTGAGGTC
	R3	GGAATGTGAAGTTATTATACCCGTTACTCGTAGAGTAACAGAACACACC
	40_bp_chc_+_20_bp_HA_F2	CCTGTAAATGCTCCTGAAAGCGGATGGGCAGTGGTTGCGTGGCGTAGTCGGGCACGTCGTAG
	F3	GGAATGTGAAGTTATTATACCCGTTACTCGTAGAGTAACAGAACACACC
	HA_middle_R	GCGCCCATGTCGCGGCCGCTGTAATCCTTCGATTACATCGTTACCTCACGGCGATAATCTTG

F, forward; R, reverse.

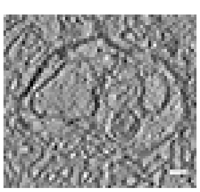

Video 1. **Electron tomogram of stimulated *shi*$^{12\text{-}12B}$/Y; *shi-4C*/+ larvae at restrictive temperature after FALI.** Video shows an electron tomogram of a stimulated bouton of *shi*$^{12\text{-}12B}$/Y; *shi-4C*/+ larvae at restrictive temperature after FALI. A tilt series of a 300-nm-thick section was collected from −52 to 60° with 2° angular increments in a transmission electron microscope (JEM-2100; JEOL) at 10,000× using Recorder software (JEOL) and a 1,024 × 1,024–pixel bottom-mounted charge-coupled device camera (MultiScan; Gatan). Tomograms were reconstructed with the eTomo module in IMOD. Each video frame in the tomogram is an individual slice (54 slices in total). The surface-rendered model, built by semiautomated surface rendering and computed using 3dmod in IMOD, is shown in Fig. 7. Note the accumulation of membrane inclusions that are also connected to the presynaptic membrane. Bar, 200 nm.